Inverse Scattering Tridiagonal NN Potentials and Few-Nucleon Systems.

A. M. Shirokov*, A. I. Mazur†, S. A. Zaytsev†, J. P. Vary‡ and T. A. Weber‡

*Skobeltsyn Institute of Nuclear Physics, Moscow State University, Moscow, 119992, Russia

†Physics Department, Khabarovsk State Technical University, Tikhookeanskaya 136, Khabarovsk 680035, Russia

‡Department of Physics and Astronomy, Iowa State University, Ames, Ia 50011-3160, USA

Abstract

The nucleon-nucleon interaction is constructed by means of the J-matrix version of inverse scattering theory. Ambiguities of the interaction are eliminated by postulating tridiagonal and quasi-tridiagonal forms of the potential matrix in the oscillator basis in uncoupled and coupled waves, respectively. The obtained interaction is very accurate in reproducing the NN scattering data and deuteron properties. The interaction is used in the no-core shell model calculations of ^{3}H and ^{4}He nuclei. The resulting binding energies are very close to experimental values.

1 Introduction

The nucleon-nucleon (NN) interaction is one of the most important ingredients in microscopic nuclear structure calculations. Ideally, the NN interaction should be derived from the quark-gluon theory. However, the QCD-based derivation of the NN potential for low energy applications is impossible at this time.

NN potentials conventionally referred to as '*realistic*', are derived from the meson exchange theory. Modern realistic NN potentials like Bonn [1], Argonne [2], Nijmegen [3], etc., are carefully fitted to the existing experimental data on NN scattering and deuteron properties. Unfortunately, none of the known NN interactions provides a completely satisfactory description of the trinucleon and other light nuclei. To overcome this deficiency, either semi-realistic [4] or phenomenological [5] three-nucleon (NNN) forces are usually introduced. Impressive progress was achieved recently in the description of the trinucleon and ^{4}He binding energies with realistic NN and three-nucleon forces [6]. However, there are concerns about the consistency between NN and NNN potentials. In one very detailed study, when the NNN interaction parameters were chosen consistently with the NN parameters, the NNN force contribution to the triton binding energy was shown to be negligible [7].

Impressive progress using effective field theory has recently been reported (see review in Ref. [8]). The versions that provide the most accurate fit to NN properties [9] use a momentum-space cutoff and are still quite strong at short distances. The match with the nuclear many body model space cutoff is unclear and these interactions require additional renormalization for typical model spaces that are feasible. We aim to have high quality descriptions of the phase shifts with softer potentials whose cutoff is well-matched to the anticipated application in many-body systems.

Various microscopic approaches have been designed for the studies of few-body systems. It was demonstrated in Ref. [10] that all modern microscopic methods provide approximately the same results for the ^{4}He ground state for a given realistic interaction. The no-core shell model [11, 12] is one of these methods and it can also be used for microscopic studies with modern computer facilities of heavier nuclei with the number of nucleons A up to $A \sim 12$ [12]. The no-core shell model is based on a wave function expansion in a many-body oscillator function series. It aims to describe bound states and narrow resonances treated as bound states.

Realistic NN potentials have strong correlations and cannot be directly used without a severe truncation in the many-body no-core shell model calculations. As a result, the convergence of the calculations with increasing model space is slow. This deficiency is conventionally addressed by constructing the so-called *effective NN interaction* (see, e. g., [12]). Ideally, the effective NN interaction in the finite model space should reproduce the results of the infinite model space calculation. In a realistic application, the construction of the effective NN interaction may not be adequate and effective many-body terms may need to be included.

In this contribution, we construct the NN interaction by means of the J-matrix version of inverse scattering theory [13, 14, 15]. The matrix of the NN potential in the oscillator basis is obtained for each partial wave independently. Therefore, in our approach, we derive the NN interaction as a set of potential matrices for different partial waves. Our NN interaction can be treated as an effective interaction since its matrices are small and can be directly used in the no-core shell model calculations without additional truncation. Nevertheless, our effective NN interaction reproduces the deuteron properties and NN scattering data. From this point of view our NN interaction can be treated as realistic. Our interaction is not based on meson exchange theory, however we obtain the deuteron and scattering wave functions that are very close to the ones obtained with realistic meson exchange potentials.

The potential derived by the J-matrix inverse scattering approach is ambiguous. The ambiguity originates from the phase-equivalent transformation suggested in Ref. [16] (see also [17] and references therein). The ambiguity is eliminated in the present approach by an ansatz that the potential matrix in the uncoupled partial waves is tridiagonal. Therefore we call our potentials *Inverse Scattering Tridiagonal Potentials* (ISTP). The non-central nature of the NN interaction manifests in the coupling of some partial waves, and the tridiagonal potential ansatz should be extended to allow for the coupling of these partial waves. For this case we postulate a simple generalization of the tridiagonal form of the potential matrix. We refer to our potentials as ISTP in the cases of both uncoupled and coupled partial waves (though, strictly speaking, it is not correct in the later case). It is encouraging that the tridiagonal ansatz produces scattering wave functions which are very close to the ones provided by the meson exchange realistic NN potentials. In addition, in the case of the coupled sd waves we perform a phase equivalent potential transformation to improve the description of the deuteron properties.

The suggested ISTP are used in the no-core shell model calculations of ^{3}H and ^{4}He. We do not use three-nucleon interactions, yet our predictions of the ^{3}H and ^{4}He bindings are approximately of the same accuracy as the predictions based on the best realistic meson exchange NN plus NNN forces.

2 ISTP NN potentials

The method of construction of the ISTP NN interaction is discussed in detail in Ref. [18]. We use, as an input, the np scattering phase shifts reconstructed from the experimental data by the Nijmegen group [3] and the oscillator basis parameter $\hbar\omega = 40$ MeV. In the shell model calculations, the complete $\varkappa\hbar\omega$ model space is usually used, i. e. all many-body oscillator basis states (configurations) with the oscillator quanta $N = 2n + l \leq \varkappa$ (l is the orbital angular momentum, n is the principal quantum number) are allowed in the calculation. Thus, to be applicable to all p-shell nuclei in accessible model spaces, we calculated the $8\hbar\omega$ ISTP in the partial waves with even orbital angular momentum l and $7\hbar\omega$ ISTP in the partial waves with odd orbital angular momentum l. This means, for example, that the ISTP in the uncoupled p waves is a tridiagonal 4×4 matrix ($2n+1 \leq 7$, hence n takes 4 values $n = 0, 1, 2, 3$).

The tensor components of the NN interaction couple some of the partial waves. The sd coupled partial waves (the coupling of the $^3s_1$ and $^3d_1$ partial waves) and pf coupled partial waves (the coupling of the $^3p_2$ and $^3f_2$ partial waves) are of special interest for applications. As in the case of uncoupled partial waves, we construct $8\hbar\omega$ ISTP in the coupled sd waves and $7\hbar\omega$ ISTP in the coupled pf waves. Due to the $\varkappa\hbar\omega$ restriction, the ranks N_p and N_f of the p wave and f wave diagonal submatrices of the pf ISTP are related as $N_p = N_f + 1$; in the case of sd ISTP we have the same relation between the ranks of the diagonal s wave and d wave submatrices: $N_s = N_d+1$. Thus the ISTP matrix $V_{nn'}^{\Gamma\Gamma'}$ has the following structure: the submatrices $V_{nn'}^{\Gamma\Gamma}$ coupling the oscillator components of the same partial wave are square while the submatrices $V_{nn'}^{\Gamma\Gamma'}$ with $\Gamma \neq \Gamma'$ coupling the oscillator components of different partial waves are $(N_\Gamma+1)\times N_\Gamma$ or $N_\Gamma\times(N_\Gamma+1)$ matrices. Our assumptions are: we adopt (i) the tridiagonal form of the square submatrices $V_{nn'}^{\Gamma\Gamma}$ and (ii) the simplest two-diagonal form of the non-square submatrices $V_{nn'}^{\Gamma\Gamma'}$ with $\Gamma \neq \Gamma'$ coupling the oscillator components of different partial waves. The structure of the ISTP matrices in coupled partial waves is illustrated by Fig. 1.

The resulting ISTP perfectly describe the phenomenological scattering data. In the case of the coupled sd waves, it is very important also to describe correctly the deuteron properties. The deuteron binding energy E_d and asymptotic normalization constants $\mathscr{A}_s$ and $\mathscr{A}_d$ are used as an input in the inverse scattering approach and hence are adequately described. However the obtained sd-ISTP of the structure presented in Fig. 1 (hereafter refered to as the Version 0), strongly underestimates the deuteron d state probability and overestimates the deuteron rms radius. To improve the description of the deuteron properties, we apply to our Version 0 ISTP a phase equivalent transformation discussed in Refs. [16, 17] that leaves unchanged the scattering observables, E_d, $\mathscr{A}_s$ and $\mathscr{A}_d$. We use the simplest form of the transformation mixing only the $|0s\rangle$ and $|0d\rangle$ basis functions. As a result of the transformation, the ISTP matrix acquires two additional non-zero matrix elements $V_{01}^{sd} = V_{10}^{ds}$. These additional matrix elements are schematically illustrated by filled circles in Fig. 2. This potential is hereafter referred to as Version 1 ISTP.

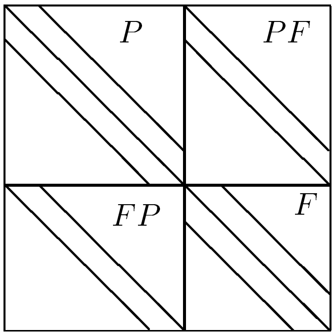

Figure 1: Structure of the ISTP matrix in the coupled pf waves and of the Version 0 ISTP in the coupled sd waves. The location of non-zero matrix is schematically illustrated by solid lines.

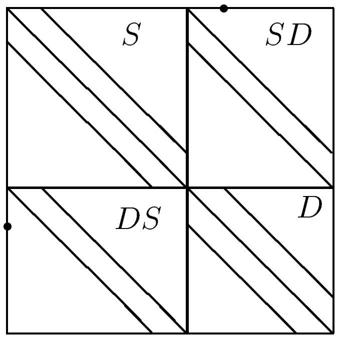

Figure 2: Structure of the Version 1 and Version 2 ISTP matrix. The location of non-zero matrix is schematically illustrated by solid lines and filled circles.

The description of the d state probability is improved by the phase equivalent transformation. However the phase equivalent transformation produces an increase of the deuteron rms radius; so this observable becomes even worse than that given by the Version 0 ISTP.

To improve the sd-ISTP we suggest a slight change to the s wave asymptotic normalization constant $\mathscr{A}_s$ that is used as an input in our inverse scattering approach. The $\mathscr{A}_s$ value cannot be measured in a direct experiment. As was mentioned in Ref. [20], the $\mathscr{A}_s$ values discussed in the literature vary within a broad range from 0.7592 fm$^{-1/2}$ to 0.9863 fm$^{-1/2}$. Therefore, the modified value $\mathscr{A}_s = 0.8629$ fm$^{-1/2}$ that we use for the construction of the improved sd-ISTP, seems to be reasonable. We do not change the remaining inputs in our inverse scattering approach including $\eta = \dfrac{\mathscr{A}_d}{\mathscr{A}_s}$ (and hence we modify $\mathscr{A}_d$ together with $\mathscr{A}_s$) to obtain the ISTP of the type shown in Fig. 1 and apply to it the phase equivalent transformation to obtain the potential (hereafter referred to as Version 2 ISTP) of the type depicted in Fig. 2. The Version 2 ISTP provides the realistic description of all deuteron properties as is seen from Table 1 where we compare the pre-

Table 1: Deuteron property predictions obtained with various $8\hbar\omega$ ISTP versions and with Nijmegen-II potential in comparison with recent compilations [19, 20].

Potential	E_d, MeV	d state probability, %	rms radius, fm	$\mathscr{A}_s$, fm$^{-1/2}$	$\eta = \dfrac{\mathscr{A}_d}{\mathscr{A}_s}$
Version 0	2.224575	0.4271	1.9877	0.8845	0.0252
Version 1	2.224575	5.620	1.9997	0.8845	0.0252
Version 2	2.224575	5.696	1.968	0.8629	0.0252
Nijmegen-II	2.224575	5.635	1.968	0.8845	0.0252
[19]	2.224575(9)	5.67(11)	1.9676(10)	0.8845(8)	0.0253(2)
[20]	−2.224589	—	$\begin{cases} 1.9635 \\ 1.9560 \\ 1.950 \end{cases}$	0.8781	0.0272

dictions of the Version 0–2 ISTP with the ones obtained with Nijmegen-II potential and with recent compilations of the experimental data [19, 20]. The deuteron wave functions are presented in Fig. 3.

As we have already mentioned, our potentials provide a very good description of the experimental scattering data. As an example we present in Figs. 4–6 the plots of the phase shifts δ_s and δ_d and of the mixing parameter ε in the coupled sd waves. The data are seen to be reproduced with a high accuracy. In other coupled and uncoupled partial waves the experimental phase shifts are reproduced with approximately the same accuracy.

It is interesting that ISTP give rise to the scattering wave functions that are very close to the ones obtained with realistic meson exchange potentials as is seen from Figs. 7–8

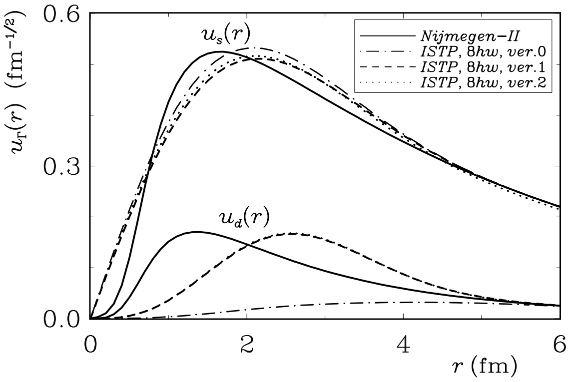

Figure 3: Radial deuteron wave functions. Solid line — realistic meson exchange Nijmegen-II potential [3] wave functions; dot-dash line — Version 0 ISTP wave functions; dashed line — Version 1 ISTP wave functions; dotted line — Version 2 ISTP wave functions.

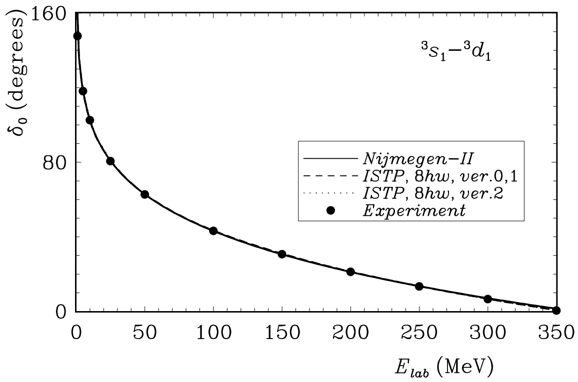

Figure 4: $^3s_1$ np scattering phase shifts δ_s (coupled sd waves). Filled circles — experimental data of Ref. [3]; solid line — realistic meson exchange Nijmegen-II potential [3] phase shifts; dashed line — Version 0 and Version 1 ISTP phase shifts; dotted line — Version 2 ISTP phase shifts.

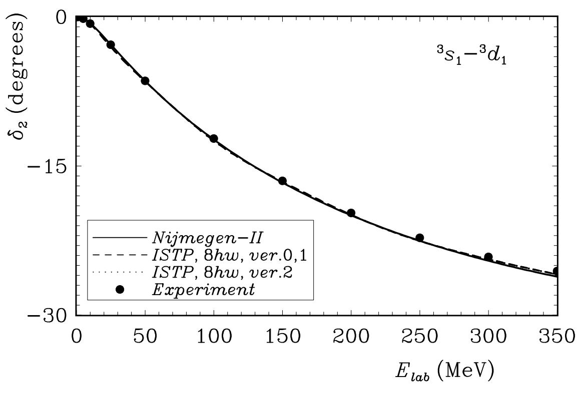

Figure 5: $^3d_1$ np scattering phase shifts δ_d (coupled sd waves). See Fig. 4 for details.

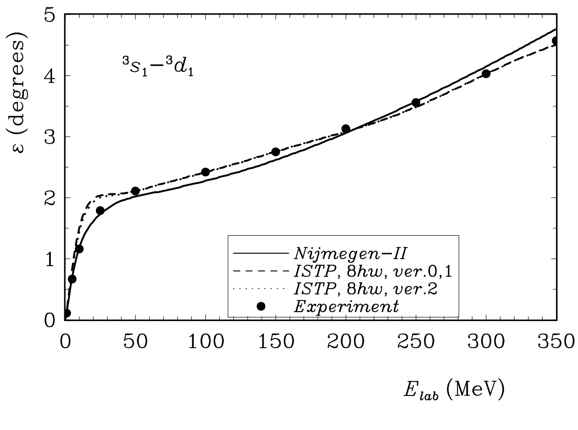

Figure 6: np scattering mixing parameter ε in the coupled sd waves. See Fig. 4 for details.

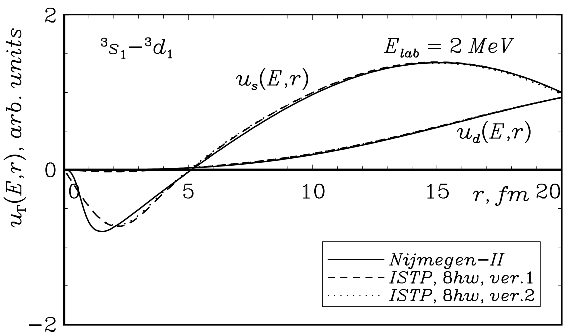

Figure 7: s wave and d wave components of the coupled sd waves np scattering wave function at the laboratory energy $E_{\rm lab}$ = 2 MeV. See Fig. 3 for details.

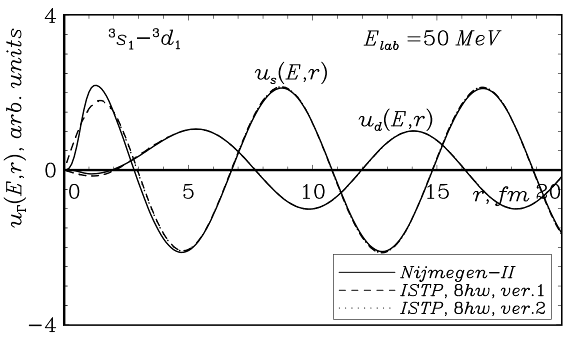

Figure 8: s wave and d wave components of the coupled sd waves np scattering wave function at the laboratory energy $E_{\rm lab}$ = 50 MeV. See Fig. 3 for details.

where we compare our np scattering wave functions at the laboratory energies $E_{\rm lab} = 2$ and 50 MeV. The ISTP scattering wave functions are very close to those of realistic meson exchange potentials in other partial waves too.

3 Few-nucleon systems bound by ISTP interaction

We employ the obtained ISTP in the ^{3}H and ^{4}He calculations within the no-core shell model [11, 12] with $\hbar\omega = 40$ MeV. The same NN potentials are used to describe the neutron-neutron and neutron-proton interactions; in the proton-proton case these potentials are supplemented by the Coulomb interaction. The calculations are performed in the complete $N\hbar\omega$ model spaces with $N \leq 14$.

We have presented various versions of ISTP in the coupled sd partial waves while ISTPs in other partial waves are held fixed. Using this fixed set of the non-sd-ISTP in combination with the Version M sd-ISTP (M = 0, 1, 2, 3), we have the set of potentials that is refered to as the Version M potential model in what follows.

The ^{3}H ground state energies E_t obtained with the Version 1 and the Version 2 potential models in $N\hbar\omega$ model spaces are presented in Fig. 9 as functions of $1/N$. It is seen that both potential models provide very similar E_t values. The convergence of the calculations with N appears adequate. The ground state energy E_t is seen from the figure to be nearly a linear function of $1/N$. Therefore it is natural to perform a linear extrapolation to the infinite $N\hbar\omega$ model space, i. e. to the point $1/N = 0$. The linear extrapolation using the two results at the highest N-values yields $E_t \approx -8.6$ MeV in the Version 1 potential model and in $E_t \approx -8.7$ MeV in the Version 2 potential model.

In Fig. 10 we present the results of the ^{4}He ground state energy E_α calculations with the same potential models. In the ^{4}He case we also obtain very similar results with the Version 1 and the Version 2 potential models. It is interesting that the convergence of the ^{4}He ground state energy is better than that of ^{3}H. In this case the curves connecting the E_α values deviate from straight lines. Nevertheless we also perform the linear extrapolations of $E_\alpha(1/N)$ to infinite N using the E_α values obtained in $12\hbar\omega$ and $14\hbar\omega$ calculations and

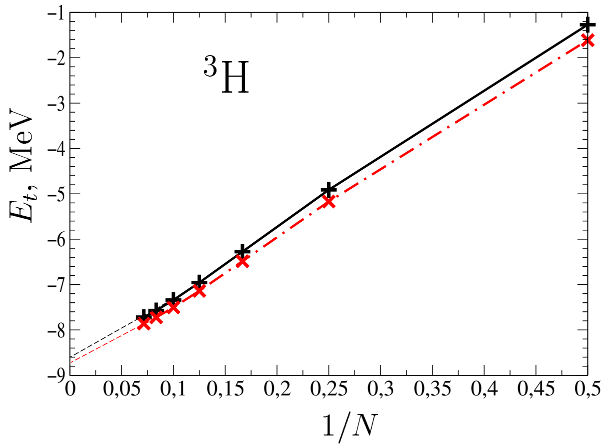

Figure 9: ^{3}H ground state energy obtained in the $N\hbar\omega$ no-core shell model calculation vs $1/N$. + — Version 1 potential model; × — Version 2 potential model; dashed line — linear extrapolation to the infinite $N\hbar\omega$ model space based on the last two calculated points ; solid and dash-dot lines are to guide the eye.

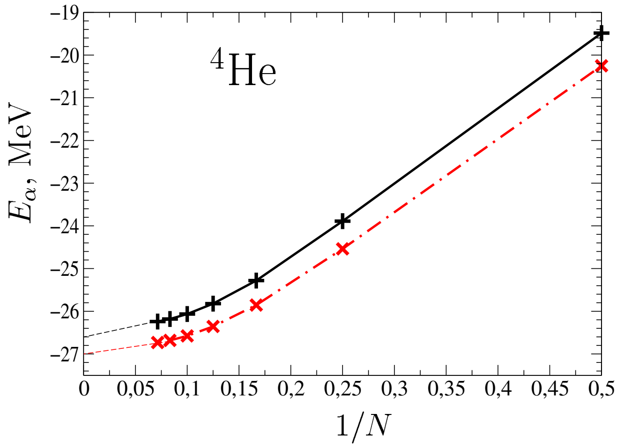

Figure 10: ^{4}He ground state energy obtained in the $N\hbar\omega$ no-core shell model calculation vs $1/N$. See Fig. 9 for details.

obtain $E_\alpha \approx -26.6$ MeV in the Version 1 potential model and $E_\alpha \approx -27.0$ MeV in the Version 2 potential model.

The differences in convergence rates for the deuteron, ^{3}H and ^{4}He can be understood from the fact that $\hbar\omega = 40 MeV$ is more optimal for the tighter bound ^{4}He than for the lesser bound systems.

Our results of the ^{3}H and ^{4}He ground state energy calculations are summarized in Table 2. We also present in the table the results obtained in the less realistic Version 0 potential model. Both ^{3}H and ^{4}He are essentially overbound in this potential model. With both Version 1 and Version 2 potential models we obtain a reasonable description of the ^{3}H and ^{4}He bindings. The ^{3}H ground state energy obtained in Faddeev calculations with CD-Bonn NN potential is -8.012 MeV (see [6]). All the remaining modern realistic meson exchange potentials predict the ^{3}H binding energy to be less than 7.4 MeV [6]. Therefore our ^{3}H binding energy predictions are not worse than those obtained with the

Table 2: ^{3}H and ^{4}He ground state energies (in MeV) obtained in $14\hbar\omega$ no-core shell model calculations and by the linear extrapolation to the infinite $N\hbar\omega$ model space.

Potential model	^{3}H		^{4}He	
	$14\hbar\omega$	extrapolation	$14\hbar\omega$	extrapolation
Version 0	-9.091	-9.7	-33.223	-33.4
Version 1	-7.718	-8.6	-26.241	-26.6
Version 2	-7.860	-8.7	-26.734	-27.0
Nature	-8.48		-28.30	

realistic meson exchange potentials without allowing for the three-body forces while our ^{4}He binding energy predictions are better. Applications to heavier nuclei are in progress.

This work was supported in part by the State Program "Russian Universities", by the Russian Foundation of Basic Research grant No 02-02-17316, by USDOE grant No DE-FG-02 87ER40371, and by US NSF grant No PHY-007-1027.

References

[1] R. Machleidt, F. Sammarruca, and Y. Song, Phys. Rev. **C 53**, 1483 (1996).

[2] R. B. Wiringa, V. G. J. Stoks, and R. Schiavilla, Phys. Rev. **C 51**, 38 (1995).

[3] V. G. J. Stoks, R. A. M. Klomp, C. P. F. Terheggen, and J. J. de Swart, Phys. Rev. **C 49**, 2950 (1994).

[4] S. A. Coon and H. K. Han, Few-Body Syst. **30**, 131 (2001); D. C. J. Marsden, P. Navrátil, S. A. Coon, and B. R. Barrett, Phys. Rev. **C 66**, 044007 (2002).

[5] B. S. Pudliner, V. R. Pandharipande, J. Carlson, S. C. Pieper, and R. B. Wiringa, Phys. Rev. **C 56**, 1720 (1997); R. B. Wiringa, Nucl. Phys. **A 631**, 70c (1998).

[6] A. Nogga, H. Kamada, and W. Glöckle, Phys. Rev. Lett. **85**, 944 (2000).

[7] A. Picklesimer, R. A. Rice, and R. Brandenburg, Phys. Rev. Lett. **68**, 1484 (1992); Phys. Rev. **C 45**, 547 (1992); Phys. Rev. **C 45**, 2045 (1992); Phys. Rev. **C 45**, 2624 (1992); Phys. Rev. **C 46**, 1178 (1992).

[8] S. R. Beane, P. F. Bedaque, W. C. Haxton, D. R. Phillips, M. J. Savage, in: M. Shifman (Ed.), *At the Frontier of Particle Physics*, Vol. 1, 133 (World Scientific); nucl-th/0008064.

[9] D. R. Entem, R. Machleidt, Phys. Lett. **B 524**, 93 (2002).

[10] H. Kamada, A. Nogga, W. Glöckle, E. Hiyama, M. Kamimura, K. Varga, Y. Suzuki, M. Viviani, A. Kievsky, S. Rosati, J. Carlson, S. C. Pieper, R. B. Wiringa, P. Navrátil, B. R. Barrett, N. Barnea, W. Leidemann, and G. Orlandini, Phys. Rev. **C 64**, 044001 (2001).

[11] D. C. Zheng, J. P. Vary, and B. R. Barrett, Phys. Rev. **C 50**, 2841 (1994); D. C. Zheng, J. P. Vary, B. R. Barrett, W. C. Haxton, and C. L. Song, Phys. Rev. **C 52**, 2488 (1995).

[12] P. Navrátil, J. P. Vary, and B. R. Barrett, Phys. Rev. Lett. **84**, 5728 (2000); Phys. Rev. **C 62**, 054311 (2000).

[13] S. A. Zaytsev, Teoret. Mat. Fiz. **115**, 263 (1998) [Theor. Math. Phys. **115**, 575 (1998)].

[14] S. A. Zaytsev, in *Proc. XIV Int. Workshop on High Energy Physics and Quantum Field Theory, Moscow 1999)* (Ed. B.B.Levchenko and V.I.Savrin), 666 (Moscow, MSU-Press, 2000); Teoret. Mat. Fiz. **121**, 424 (1999) [Theor. Math. Phys. **121**, 1617 (1999)].

[15] S. A. Zaitsev and E. I. Kramar J. Phys. **G 27**, 2037 (2001).

[16] Yu. A. Lurie and A. M. Shirokov, Izv. Ros. Akad. Nauk, Ser. Fiz. **61**, 2121 (1997) [Bull. Rus. Acad. Sci., Phys. Ser. **61**, 1665 (1997)].

[17] Yu. A. Lurie and A. M. Shirokov, nucl-th/0312028; to be published in A. D. Alhaidari, E. J. Heller, H. A. Yamani, and M. S. Abdelmonem (eds.), *J-matrix method and its applications* (Nova Science Publishers, Inc.).

[18] A. M. Shirokov, A. I. Mazur, S. A. Zaytsev, J. P.Vary, T. A.Weber, nucl-th/0312028; to be published.

[19] J. J. de Swart, C. P. F. Terheggen, and V. G. J. Stoks, *Invited talk by J. J. de Swart at the 3rd Int. Symp. "Dubna Deuteron 95", Dubna, Russia, July 4–7, 1995*; nucl-th/9509032.

[20] V. A. Babenko and N. M. Petrov, nucl-th/0307001; to be published in Phys. At. Nucl.